ORIGINAL RESEARCH PAPER
VOLUME-6 | ISSUE-7 | JULY-2017 | ISSN No 2277 - 8179 | IF : 4.176 | IC Value : 78.46
INTERNATIONAL JOURNAL OF SCIENTIFIC RESEARCH

PARAMETRIC INSTABILITY OF ROTATING CANTILEVER FUNCTIONALLY GRADED MATERIAL PLATES

Engineering

Ramu Inala Associate professor, Department of Mechanical Engineering, Vishnu Institute of Technology, Bhimavaram, Andhra Pradesh-534202

ABSTRACT

The present work deals with a finite element method for the vibration and parametric instability of rotating cantilever FGM plates, based on first order shear deformation theory. The equation of motion of rotating FGM plates are established by using Hamilton's principle and they are a set of coupled second order deferential Mathieu equation with periodic coefficients. The boundary parametric resonance frequencies of the motion are determined using Bolotin's approach. The effect of power law index value, thickness ratio, radius of hub and rotating speed on dynamic stability of plates subjected to in-plane periodic loads are investigated using finite element method. The excited frequency ratio of rotating FGM plates increase by increase the hub radius and rotational speed due to increase of overall stiffness for FGM plates. The overall enhancement of dynamic stability of the rotating cantilever FGM plates has been performed.

KEYWORDS:

Rotating cantilever plate, free vibration, functionally graded material, harmonic load, parametric instability.

1. INTRODUCTION

The contemporaneous studies on a novel advanced composite materials have introduced new materials called as functionally graded materials (FGM). This materials established considerable deliberation in structural design specifically, in which the materials are exposed to very high thermal environment. The FGM properties can be specially made to achieve the particular necessities in many applications in engineering field to attain the advantages of the individual material properties. So, it is conceivable because of the material constituents of the FGM varies constantly in desired path. Rotating plate like structures has many applications such as turbo machinery, wind blades and helicopter rotating blades. These plates are often subjected to high pressure periodic loadings. The wide range of applications of rotating plates are need to understand their vibration and parametric instability characteristics. Several rotating structures, like turbo machinery, wind blades and helicopter rotating blades are modelled as plates that are often subjected to vibration by high pressure loadings and thermo-elastically induced loadings. Due to the extensive range of applications demands a significant considerate of their vibration and parametric instability analysis of rotating FGM plates exposed to in plane periodic loadings is studied by Ramu (2015). The problem of dynamic stability in various elastic structures is studied by Bolotin (1962).

From the fast decade, many researchers have studied the vibration characteristics of rotating isotropic plates and static FGM plates using various methods. Vibration analysis of twisted rotating plates studied by Sreenivasa and Ramamurti (1981) using two different shape functions. Ramamurti and Kielb (1984) have examined the Coriolis Effect on fundamental frequencies of bending and torsional of cantilever rotating plate using finite element method. They also considered the stresses smoothing method for calculating improved stiffness matrix to reduce the numerical error. The free vibration analysis of rotating rectangular plates were presented by Wang et al. (1987). The pretwisted laminated composite cantilever plate free vibration analysis have been studied by Amit and Sinha (1997) using finite element method. Yoo and Pierre (2001) used dynamic modelling technique to examine the characteristics of a rotating cantilever plate. The flap wise bending vibration analysis of rotating plate linear governing equations of motion has been developed by Yoo et al. (2002). They expressed in a quadratic form based on strain energy of a plate with two in-plane stretch variables. The governing equation of motion based on hybrid deformation variables for free vibration analysis of rotating pre-twisted blades was derived by Yoo et al. (2003).

The Coriolis Effect considered based on Kane dynamic method ware proposed Hashemi et al. (2009) for vibration analysis of rotating thick plates. Free vibration analysis of a thin square plates were established by Saha et al. (2004) with different boundary conditions. Zhang and Zhou (2001) presented the concept of physical neutral surface of FGM thin plates. Zhao et al. (2009) presented the metal and ceramic FGM plates free vibration analysis using element-free kernel particle -Ritz method. Same others (2009) examined buckling analysis for the FG plates with the mechanical and thermal conditions using element-free Ritz method. Samsam et al. (2005) studied the buckling behavior of FG rectangular plates with geometrical imperfections.

Hosseini-Hashemi et al. (2011) studied free vibration analysis of rectangular plates using an exact closed form solution with various boundary conditions. The Same authors in (2011) provided a closed-form solution using Reddy's third order shear deformation theory for free vibration analysis of FG rectangular thick plate. An exact solution for free vibration analysis of isotropic and FGM plates studied by Efraim and Eisenberger (2007). Mohammad and Singh [2010] investigated the free vibration analysis of FGM plates using higher order shear deformation theory. Finite element approach with 13 degree of freedom per node is formed with shear deformable FG ceramic-metal plates were presented by Talha and Singh (2011) for thermo-mechanical vibration analysis.

Chih-Ping and Hao-Yuan (2014) studied the free vibration analysis of FG carbon nanotube-reinforced composite plates based on the Reissner's variational theorem. A unified formulation of finite prism method was used for solving equations. Hesham and Tawfik (2010) examined the thermal buckling and nonlinear flutter analysis of a FGM plate panel with combined thermal and aerodynamic loadings. Saeidifar and Ohadi (2011) presented the bending vibration, buckling and dynamic response of non-uniform plates with flexible parameters in one direction. They were used the Mindlin-Goodman and Frobenius methods to develop a solution for plate with general boundary conditions. Jayaram et al. (2013) have studied the delaminated composite plates parametric instability under periodic loading. Ramu and Mohanty (2015) presented the dynamic stability of FGM plates by different boundary conditions.

However, most of researchers concentrated on free vibration analysis of rotating plates with isometric and FGM materials. The present paper focus the finite element formulation and on dynamics stability of rotating cantilever FGM plates under in plane periodic loading. A FGM rectangular plate model is established using third order shear deformation theory for natural frequency, buckling and parametric instability of rotating cantilever FGM plate. The present proposed numerical results are shown the effect of power law index and thickness ratio on vibration and dynamic stability of rotating cantilever FGM plates. The natural frequency and parametric instability of rotating FGM plate plots are obtained for varying hub radius and rotating speed.

2. MATHEMATICAL FORMULATION

2.1 THE BASIC PROBLEMS

The figure 1 represents the periodic load acting on the FGM plate with one end if fixed.

$P(t)=P_s+P_t \cos\Omega t$

where static component of the axial force is P_s. The amplitude and frequency of the force dynamic component are P_t and Ω respectively,

and t is time.

The governing equation of motion of the plate is derived using finite element method by considering four noded rectangular plate element. The reference plane is chosen as neutral axis of a plate for basic kinematics expressions. The plate is fixed to the hub with a radius of R, The geometrical consideration of the plate is of length L, width W, and thickness h as shown in figure 1.

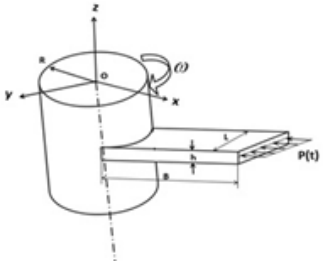

Fig.1 Rotating functionally graded material cantilever plate

2.2 FGM plate constitutive law

FGMs are novel new inhomogeneous composite materials. FGMs are made up of two or more material constitutes phases and the distributions of composition is continuously varying in one or more directions in a distinct geometry. The constituents of material properties distribution decreases the effect of the existence of interfaces and avoids interfacial stresses. A FGM plate made of top surface as alumina and bottom surface as steel is shown in figure 2. The effective material property varies from the top surface to bottom surface.

The volume division of the constituent ceramic material according to the power law can be expressed as

$$V_c = \left(\frac{1}{2} + \frac{z}{h}\right)^k, 0 \le k \le \infty \qquad (1)$$

here *k* is the index value of power law, which proposes the material properties vary along the thickness direction of the plate. where z varies from –h/2 to h/2. The top surface (*z = -h/2*) of the plate is metal-rich, whereas the bottom surface (*z =h/2*) is ceramic-rich.

From simple rule of mixture

$$V_C(Z) + V_M(Z) = 1 \qquad (2)$$

where *VC* is volume of ceramic and *VM* volume of metal, respectively. The active material properties *(P)* can be expressed as

$$P = P_c V_c + P_m V_m \qquad (3)$$



Fig. 2 Geometry of the FGM plate

2.3 FGM plate physical neutral surface

The geometric mid surface of the FGM plate may not coinside with its neutral surface, due to its densities difference. So the distance between the geometrical mid surface and neutral surface may be expressed as

$$d = \frac{\int_{-h/2}^{h/2} zE(z)dz}{\int_{-h/2}^{h/2} E(z)dz} \qquad (4)$$

It can be found that homogeneous isotropic or symmetrical composite plates the neutral surface and geometric middle surface are the same. The effective material constituent properties of FGM plates can be expressed as follows

$$E = E_m(z) + [E_c(z) - E_m(z)]\left(\frac{2z+h}{2h}\right)^k \qquad (5a)$$

$$\nu = \nu_m(z) + [\nu_c(z) - \nu_m(z)]\left(\frac{2z+h}{2h}\right)^k \qquad (5b)$$

$$\rho = \rho_m(z) + [\rho_c(z) - \rho_m(z)]\left(\frac{2z+h}{2h}\right)^k \qquad (5c)$$

2.4 KINEMATICS

The displacements of FGM plate with reference to neutral surface u, v, w at a point (x, y, z') can be expressed as:

$$\begin{aligned} u(x,y,z) &= z'\theta_x(x,y), \\ v(x,y,z) &= z'\theta_y(x,y), \\ w(x,y,z) &= w(x,y) \end{aligned} \qquad (6)$$

here the rotation of the normal in xz planes θ_x and the rotation of normal yz plane θ_y

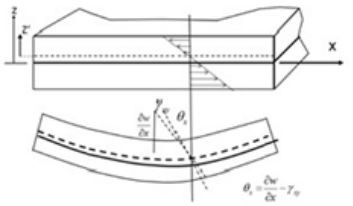

Fig.3 Plate structure before and after deformation.Displacement relations with plane strain and transverse shear strains conditions are represented as

$$\begin{bmatrix} \varepsilon_{xx} \\ \varepsilon_{yy} \\ \varepsilon_{xy} \end{bmatrix} = z' \begin{bmatrix} \frac{\partial \theta_x}{\partial x} \\ \frac{\partial \theta_y}{\partial y} \\ \frac{\partial \theta_x}{\partial y} + \frac{\partial \theta_y}{\partial x} \end{bmatrix}, \begin{bmatrix} \gamma_x \\ \gamma_y \end{bmatrix} = \begin{bmatrix} \frac{\partial w}{\partial x} + \theta_x \\ \frac{\partial w}{\partial y} + \theta_y \end{bmatrix} \qquad (8)$$

The relationship of plane stress and transverse shear stress are given as

$$\begin{bmatrix} \sigma_x \\ \sigma_y \\ \sigma_{xy} \end{bmatrix} = z' D_b \begin{bmatrix} \varepsilon_{xx} \\ \varepsilon_{yy} \\ \varepsilon_{xy} \end{bmatrix} \begin{bmatrix} \tau_x \\ \tau_y \end{bmatrix} = D_s \begin{bmatrix} \gamma_x \\ \gamma_y \end{bmatrix} \qquad (10)$$

where

$$D_b = \frac{Eh^3}{12(1-\nu^2)} \begin{bmatrix} 1 & \nu & 0 \\ \nu & 1 & 0 \\ 0 & 0 & \frac{1-\nu}{2} \end{bmatrix}, D_s = \frac{Ehk_{sh}}{2(1-\nu)} \begin{bmatrix} 1 & 0 \\ 0 & 1 \end{bmatrix}$$

The equations for bending moment and shear force relationships are defined as

$$\begin{bmatrix} M_x \\ M_y \\ M_{xy} \end{bmatrix} = \int_{-h/2-d}^{h/2-d} \begin{bmatrix} \sigma_x \\ \sigma_y \\ \sigma_{xy} \end{bmatrix} z' dz' = \begin{bmatrix} \theta_{x,x} \\ \theta_{y,y} \\ \theta_{x,y} + \theta_{y,x} \end{bmatrix} \int_{-h/2-d}^{h/2-d} D_b z'^2 dz' \qquad (11)$$

$$\begin{bmatrix} Q_x \\ Q_y \end{bmatrix} = \int_{-h/2-d}^{h/2-d} \begin{bmatrix} \tau_x \\ \tau_y \end{bmatrix} dz' = \begin{bmatrix} w_x + \theta_x \\ w_y + \theta_y \end{bmatrix} \int_{-h/2-d}^{h/2-d} D_s dz' \qquad (12)$$

2.5 ENERGY EQUATIONS

The stress resultants and strain components of the plate element potential strain energy U^e through integrating by parts with respect to coordinates can be expressed as

$$U^e = U^e_{pe} + U^e_t \qquad (13)$$

where U^e_{pe} is plane stress strain energy contribution

and U^e_t is transverse shear stress strain energy contribution.

$$U^e = \frac{1}{2}\int_a \int_{-h/2-d}^{h/2-d} \left[\varepsilon_x \;\; \varepsilon_y \;\; \varepsilon_{xy}\right] D_b \begin{pmatrix}\varepsilon_x\\ \varepsilon_y\\ \varepsilon_{xy}\end{pmatrix} dz\,dx + \frac{k_{sh}}{2}\int_a \int_{-h/2-d}^{h/2-d} \left[\gamma_{xz} \;\; \gamma_{yz}\right] D_s \begin{pmatrix}\gamma_{xz}\\ \gamma_{yz}\end{pmatrix} dz\,dx \qquad (14)$$

here k_{sh} is shear correction factor,

$$k_{sh} = \frac{5}{6-\left(\upsilon_m V_m + \upsilon_c V_c\right)}$$

V_m and V_c presents the volume fraction of metal and ceramic, υ_m and υ_c stands the Poisson ratios of metal and ceramic.

As the plate is subjected to external axial in-plane load, it subsequently produces in-plane stress resultants. Hence, the work done by the in-plane forces of plate element as follows

$$W^e_g = \frac{1}{2}\left(\int_A N_x \left(\frac{\partial w}{\partial x}\right)^2 dx + \int_A N_y \left(\frac{\partial w}{\partial y}\right)^2 dy\right) \qquad (15)$$

where N_x and N_y are the axial in-plane forces.

When plate is rotating subsequently it produces centrifugal forces. Therefore, the work done by the plate due to rotating speed is expressed as

$$W^e_c = \frac{1}{2}F^e_c w^2 dx = \frac{1}{2}\left\{q^e\right\}^T \left[k_c\right]^e \left\{q^e\right\}$$

The elemental centrifugal force of the plate element as fallows

$$F^e_c = \int_{x_i}^{x_i+l} \int_{-h/2-d}^{h/2-d} b\rho\left(z'\right)\Omega^2\left(R+x\right)dz'dx \qquad (16)$$

where *xi* is the distance of ith node from axis of rotation, angular velocity of plate element is *Ω (rad/s)* and radius of hub R.

The kinetic energy of the plate element follows as

$$T^e = \frac{1}{2}\iint_A \rho h\dot{w}^2 dA \qquad (17)$$

2.6 FINITE ELEMENT APPROACH

The present proposal of the problem considering three DOFs *w, θx,* and *θy.* Finite element modelling with a four-noded rectangular element is employed. In the FE formulation, the area is discretised into a defined set of finite elements. For each element, the geometry of the model and the displacement vector is expressed as

$$w = \sum_{i=1}^{n} N_i w_i$$
$$\theta_x = \sum_{i=1}^{n} N_i \theta_x^i \qquad (18)$$
$$\theta_y = \sum_{i=1}^{n} N_i \theta_y^i$$

where, *n* number of nodes in the element, *Ni* are the shape functions

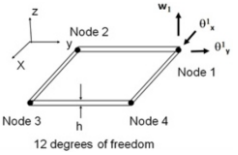

Fig.4 Finite element model of the rectangular element.

The FGM plate element strain energy is given by

$$U^e = \frac{1}{2}\left\{q^{(e)}\right\}^T \left[K_s^{(e)}\right]\left\{q^{(e)}\right\} \qquad (19)$$

where $\left\{q^{(e)}\right\}$ and $\left[K_s^{(e)}\right]$ are defined as displacement vector of the element and element stiffness matrix, respectively.

The element stiffness matrix is expressed as

$$K_s^{(e)} = \int_v [B_b]^T [D_b][B_b]dv + \int_v [B_s]^T [D_s][B_s]dv \qquad (20)$$

where

$$[B_b] = \begin{bmatrix} 0 & \frac{\partial}{\partial x} & 0 \\ 0 & 0 & \frac{\partial}{\partial y} \\ 0 & \frac{\partial}{\partial y} & \frac{\partial}{\partial x} \end{bmatrix}[N_i], [B_s] = \begin{bmatrix} \frac{\partial N_i}{\partial x} & N_i & 0 \\ \frac{\partial N_i}{\partial y} & 0 & N_i \end{bmatrix}$$

Work done due to axial in plane force

$$\left[W_g\right]^{(e)} = \int \left\{q^{(e)}\right\}^T \left[K_g^{(e)}\right]\left\{q^{(e)}\right\}dA \qquad (21)$$

here $\left[K_g^{(e)}\right]$ is defined as the geometric element stiffness matrix.

The geometric stiffness matrix for an element is expressed as

$$\left[K_g^{(e)}\right] = N_x \iint \left(\frac{\partial^2 w}{\partial x^2}\right)dxdy + N_x \iint \left(\frac{\partial^2 w}{\partial y^2}\right)dxdy$$

Here N_x and N_y are axial force along x and y axis.

The rotating cantilever FGM plate subjected to axial in plane force equation of motion is obtained by using Hamilton's principle.

$$\delta\int_{t_1}^{t_2}\left(U^e - T^e + W^e\right)dt = 0 \qquad (24)$$

In terms of element displacement vector the potential energy and the kinetic energy for an element can be written as

$$U^e = \frac{1}{2}\left\{q^e\right\}^T\left(\left[K_s^{(e)}\right] + \left[K_c^{(e)}\right]\right)\left\{q^e\right\} - \frac{1}{2}\left\{q^e\right\}^T P(t)\left[K_g^{(e)}\right]\left\{q^e\right\} \qquad (25)$$

$$T^e = \frac{1}{2}\left\{q^e\right\}^T \left[M^{(e)}\right]\left\{q^e\right\} \qquad (26)$$

The governing equation of motion for an element can be expressed as

$$\left[M^{(e)}\right]\left\{\ddot{q}^{(e)}\right\} + \left[K_{ef}^{(e)}\right]\left\{q^{(e)}\right\} - P(t)\left[K_g^{(e)}\right]\left\{q^{(e)}\right\} = 0 \qquad (27)$$

where $\left[K_{ef}^{(e)}\right] = \left[K_s^{(e)}\right] + \left[K_c^{(e)}\right]$ is effective stiffness matrix and $\left\{q^{(e)}\right\}$ is the vector of degrees of freedoms for element. The in-plane harmonic load

$P(t)$ can be expressed in the form: $P(t) = P_s + P_t \cos \Omega t$

$$\left[M^{(e)}\right]\left\{\ddot{q}^{(e)}\right\} + \left[\left[K_s^{(e)}\right] - P_{cr}(\alpha + \beta \cos \Omega t)\left[K_g^{(e)}\right]\right]\left\{q^{(e)}\right\} = 0$$

where α and β are the static and dynamic load factors respectively, and P_{cr} is the static critical buckling load of metallic plate having applied boundary conditions.

The final governing equation of motion of the rotating plate after assembly is in the form of the global displacement matrix obtained as follows $[M]\{\ddot{q}\} + [K_{ef}] - P_{cr}(\alpha + \beta \cos \Omega t)[K_g]\{q\} = 0$ (28)

where $[M]$, $[K_{ef}]$ and $[K_g]$ are global mass, global effective stiffness and global geometric stiffness matrices respectively and $\{q\}$ is global displacement vector.

The Equation (28) characterizes a system of differential equations with periodic coefficients of the Mathieu-Hill type. The regions of instability developed from Floquet's theory which solve the existence of periodic solutions of periods T and 2T.

For practical importance the condition for existence (Ω=2ω) of these boundary solutions with period 2T can be accomplished in the form of the trigonometric series:

$$q(t) = \sum_{b=1,3,..}^{\infty}\left[\{c_b\}\sin\frac{b\Omega t}{2} + \{d_b\}\cos\frac{b\Omega t}{2}\right] \quad (29)$$

In the equation the sine and cosine coefficient terms leads to a series of algebraic equations to determination of instability regions with the vectors $\{c_b\}$ and $\{d_b\}$. When b=1 represents the principal instability regions for practical attention. The principal instability conditions are resolute by the Bolotin [1962] method and improved to consider rotating cantilever plate subjected to periodic loadings.

$$\left([K_{ef}] - (\alpha \pm \beta/2)P_{cr}[K_g] - \frac{\Omega^2}{4}[M]\right)\{q\} = 0$$

The above equation gives the solution for stability and instability boundaries

$$\left|[K_{ef}] - (\alpha \pm \beta/2)P_{cr}[K_g] - \frac{\Omega^2}{4}[M]\right|\{q\} = 0 \quad (30)$$

The plus and minus sign of two conditions are corresponds to upper boundary and lower boundary of the parametric instability region.

The equation (30) reduces to number of correlated problems as show in below:

Free Vibration analysis of plate: here α=0, β=0 and Ω=2ω

$$\left|[K_{ef}] - \lambda[K_g]\right|\{q\} = 0$$

4. RESULTS AND DISCUSSION

4.1. COMPARISON STUDIES

Mathematical experiments are carried out for flapwise bending vibration of rotating cantilever isotropic plates using finite element formulation to predict the effectiveness of the present method. As the first example, the correctness of the present proposed method is shown by comparing its numerical results of those obtained by Yoo and Kim [2002]. Results for natural frequency parameter of rotating cantilever plates are tabulated in Table 1. Included in the table is also predictions of Yoo and Kim [2002] which are in good agreement with the present work.

The parameters in tables and figures δ ς ι ϖ are denote length to width aspect ratio, hub radius to length ratio, dimensionless rotation speed, thickness ratio and natural frequency parameter respectively, and are defined as expressed:

$\delta = L/B, \varsigma = R/L, \lambda = \Omega T, \iota = h/L$

$\varpi = \omega L^2\sqrt{\rho h/D}$, where

$D = Eh^3/12(1-\nu^2)$

Table 1 Compression of first five natural frequencies parameter by the present and Ref. [20] $\delta = 1, \varsigma = 0$

Dimensionless angular speed	Mode	Yoo and Kim [2002]	Southwell method	Present method
λ =1	1	3.65280	3.65427	3.7567
	2	8.64590	8.64350	8.7205
	3	21.53372	21.55690	21.6360
	4	27.38478	27.47469	27.2818
	5	31.21853	31.38484	31.0489
λ =2	1	4.11312	4.112807	4.1190
	2	9.00317	8.98438	9.4010
	3	21.96654	22.01202	22.1913
	4	27.62312	27.86609	28.1300
	5	31.58544	32.17962	31.6746

Table 2 Compression of first five natural frequencies parameter by the present and ref. [5] $\delta = 1, \varsigma = 1$

Dimensionless angular speed	Mode	Yoo and Kim [2002]	Southwell method	Present method
λ =1	1	3.86185	3.80871	3.9703
	2	8.73585	8.72801	9.1854
	3	21.71968	21.74132	21.9558
	4	27.42572	27.62624	27.9096
	5	31.36240	31.77682	31.4956
λ=2	1	4.81385	4.63956	5.1079
	2	9.34355	9.30544	10.9537
	3	22.79012	22.72604	23.7636
	4	27.79012	28.45908	29.9878
	5	32.14933	33.68323	33.0389

The next comparative study is determined to natural frequencies of FGM plates with all sides simply supported and all sides clamped boundary condition. Tables 2 and 3 validate the natural frequency parameter of FGM plates with fully simply supported and clamped edges, respectively. As shown in these tables, the present finite element results show good agreement with the previous numerical results Mohammad and Singh [2010] published in the literature for free vibration of FGM plates with different boundary conditions. The present numerical results are over predicted, it is due to the higher order displacement functions are used in reference results.

Table.1 Variation of the frequency parameter (ϖ) with the volume fraction index n for (CCCC) square (Al/Al_2O_3) FGM plates (a/h = 10)

	Ceramic		n=0.5		n=1		n=5	
S.N.	Ref. [10]	Present	Ref. [10]	Present	Ref. [10]	Present	Ref. [10]	Present
1	3.41	3.46	3.089	3.11	2.94	2.88	2.71	2.25
2	6.70	6.68	6.078	5.99	5.78	5.55	5.29	4.33
3	6.70	6.68	6.078	5.99	5.78	5.55	5.29	4.33
4	9.46	9.28	8.593	8.33	8.17	7.72	7.44	6.02
5	11.6	11.2	10.57	10.0	10.0	9.34	9.11	7.29

Table.2 Variation of the frequency parameter (λ) with the volume fraction index n for (SSSS) square (*Al/Al2 O3*) FGM plates (a/h = 10)

	Ceramic		n=0.5		n=1		n=5	
S.N.	Ref.[10]	Present	Ref.[10]	Present	Ref.[10]	Present	Ref.[10]	Present
1	1.93	1.96	1.75	1.76	1.685	1.63	1.569	1.27
2	4.72	4.75	4.26	4.26	4.060	3.95	3.765	3.08
3	4.72	4.75	4.26	4.26	4.060	3.95	3.765	3.08
4	7.27	7.24	6.58	6.50	6.275	6.02	5.786	4.70
5	9.11	9.00	8.27	8.07	7.876	7.48	7.049	5.84

4.2 NATURAL FREQUENCIES OF ROTATING FGM CANTILEVER PLATES

The present proposed finite element methodology is employed to study the free vibration, buckling and parametric instability of rotating cantilever FGM plates. Mathematical results are presented on the natural frequency and buckling of rotating cantilever FGM plate with

various parameters.

The FGM plate material properties are shown below:

SUS304, $\rho = 7{,}800\ kg/m^3$, $E = 201 \times 10^9\ Pa$,

$\vartheta = 0.3$

Al_2O_3, $\rho = 2{,}707\ kg/m^3$, $E = 380 \times 10^9\ Pa$, $\vartheta =$ 0.3

The variation of first and second natural frequency parameter verses length to thickness ratio (L/h) for rotating cantilever FGM plates is plotted in fig. 5 (a) and 5(b). These figures are plotted for square FGM plates, for different power law indices at rotational speed parameter and hub radius ratio . $\varsigma = 0$ In these figures the first and second frequency parameter increases with increasing the length to thickness ratio. Moreover, the increase in thickness ratio and reduce in the power law index, increase the 1st and 2nd natural frequency parameter.

Fig. 6 (a) and 6(b) illustrates the influence of hub radius to length ratio on first and second mode natural frequency parameters of rotating cantilever FGM plates. In this case square FGM plate with thickness is 0.05m and rotational speed $\lambda = 1$ considered for different power law index values. When the hub radius to length ratio increases, increase the first and second frequency parameter of rotating FGM plates.

Fig. 7(a) and 7(b) show the first and second natural frequency parameter verses rotational speed parameter. The results are related to different power law index values as shown in fig. 7(a) and 7(b), respectively. From these plots, it can be observed that the first and second frequency parameter increases with an increasing the rotational speed parameter.

The frequency parameter reduction is observer due to increase of power law index, irrespective of thickness ratio, hub radius ratio and rotational speed. The percentage of metal is increase with an increase of power law index, similarly the ceramic content is decreases. The increase in power

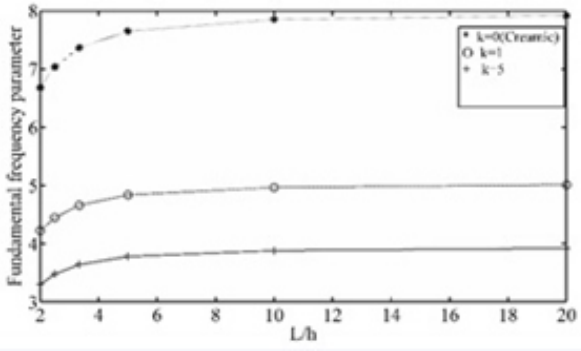

Fig. 5(a) Variation of non-dimensional first mode frequency of rotating FGM plate with thickness ratio with property distribution along

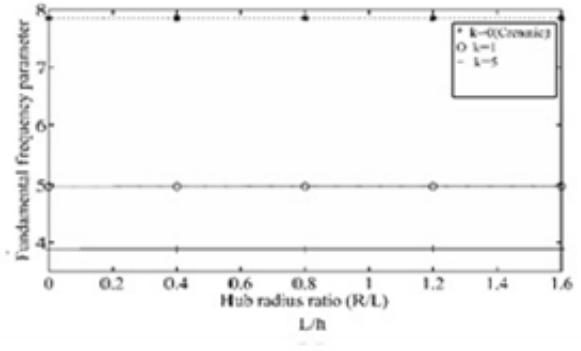

Fig. 6(a) Rotating FGM plate first mode frequency parameter variation with hub radius ratio.

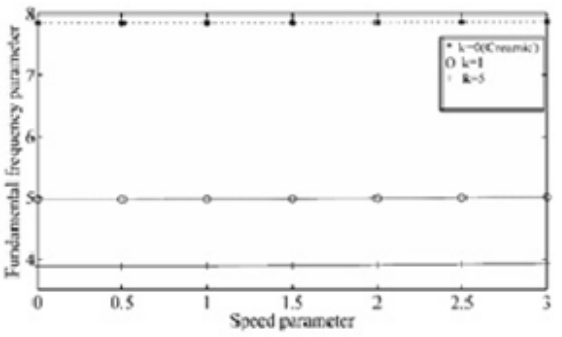

Fig. 7(a) Variation of non-dimensional first mode law index decrease the overall stiffness of rotating plate it may cause to reduction in frequency parameter.

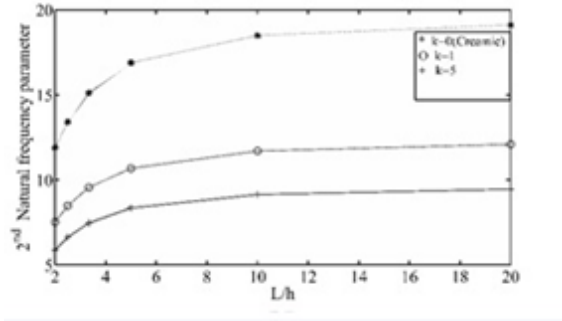

Fig. 5(b) Variation of non-dimensional second mode frequency of rotating FGM plate with thickness ratio with property distribution along thickness according to power law.

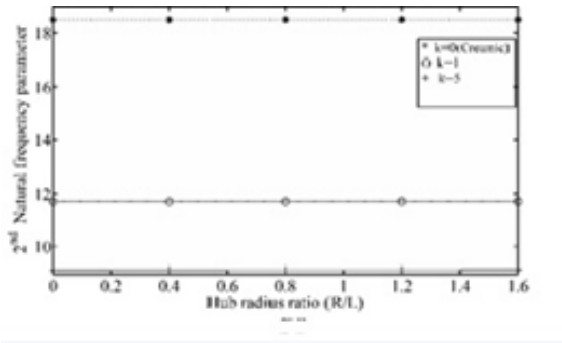

Fig. 6(b) Rotating FGM plate second mode frequency parameter variation with hub radius ratio.

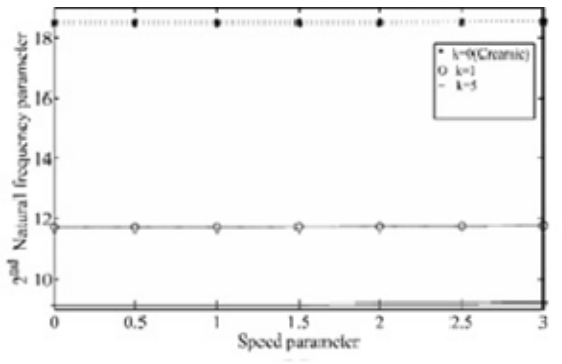

Fig. 7(b) Variation of non-dimensional second mode frequency of rotating FGM plate with rotational speed parameter.

4.3 NUMERICAL RESULTS FOR DYNAMIC STABILITY OF ROTATING CANTILEVER

FGM PLATES.

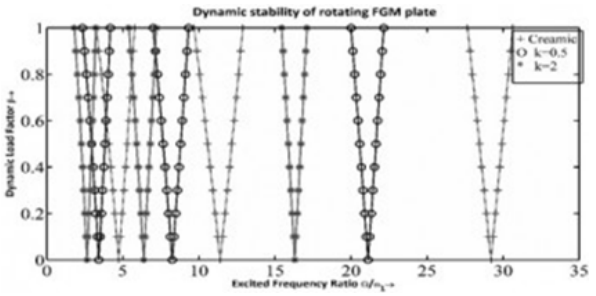

Figure. 8 Effect of property distribution power law (ceramic k=0, k=0.5 and k=2) on dynamic instability regions of rotating FGM cantilever plate

The geometrical properties of the rotating FGM plate are as follows: L/B=1, R=0.5m, h=0.05m and rotational speed (λ =1) kept constant. The difference of excitation frequency ratio with dynamic load factor of rotating cantilever FGM plate with different power law index values (Ceramic k=0, k=0.5 and k=2). It is perceived that the rise of power law index value from ceramic k=0, k=0.5 and k=2, frequency of rotating FGM plate with rotational speed parameter.

1. Effects of property distribution (k)

excited frequency ratio is reduced. The instability occurs at lower excited frequency ratio with increasing index value. The width of instability region for rotating FGM plates is reduces by increasing power law index. The overall enhancement of dynamic stability of rotating FGM plate is show in fig. (8).

2. Effect of thickness ratio (ηh/L)

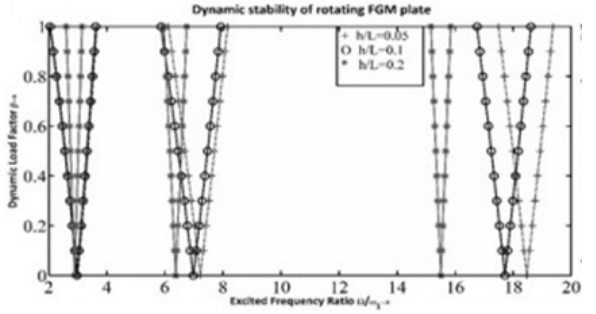

Figure.9 Dynamic stability of rotating cantilever FGM plate with different thickness ratios (h/L=0.05, 0.1 and 0.2)

The dimensions of the rotating FGM plate with L/B=1, R=0.5m, k=1 and rotational speed ($\lambda = 1$) are considered for this analysis. The excited frequency ratio verse dynamic load factor variation for rotating FGM plates subjected axial periodic loads are shown in fig.(9). The effect of thickness to length ratio is studied for h/L=0.05, 0.1, 0.2 the other geometrical and material properties kept as constant. It is observed from the dynamic stability plot the increasing thickness ratio reduces the first mode instability region width, second and third mode instability regions are change towards the dynamic load axis.

3. Effect of hub radius ratio ς

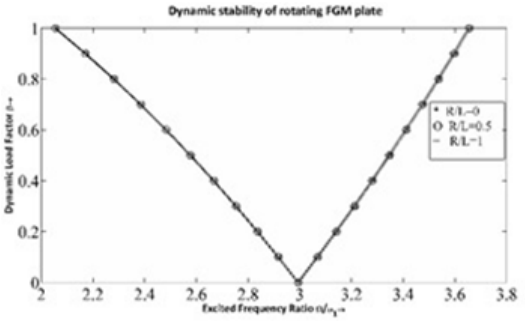

Fig. 10(a) Effect of hub radius parameter on first mode instability regions of rotating FGM plate.

geometrical and material properties kept as constant. It is observed from the dynamic stability plot the increasing thickness ratio reduces the first mode instability region width, second and third mode instability regions are change towards the dynamic load axis.

3. Effect of hub radius ratio (ς)

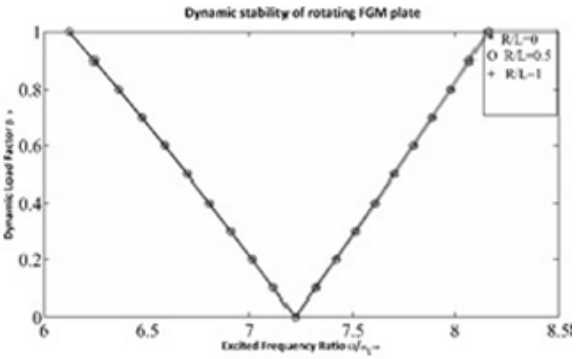

Fig. 10(b) Effect of hub radius parameter on second mode instability regions of rotating FGM plate.

The geometrical properties of the rotating FGM plates with L/B=1, R=0.5m, h=0.05m and rotational speed $\lambda = 1$ kept as constant for this study. The deviation of excited frequency ratio by dynamic load factors of rotating cantilever FGM plate subjected to periodic loads are shown in figures 10(a) and 10(b). The influence of the hub radius ratio on dynamic instability regions is studied with

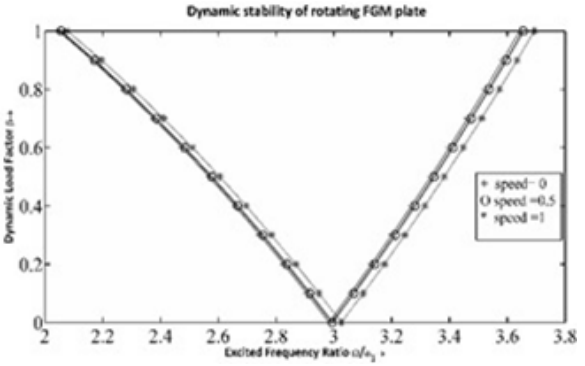

Fig. 11(a) Effect of rotating speed parameter (λ = 0, 0.5, 1) on first mode instability regions of rotating FGM plate.

The material properties of FGM plates are varying through the thickness direction according to power law by index k=1 is considered for parametric instability analysis. The effect of rotational speed on the main instability region for first and second mode are illustrated in figures 11(a) and 11(b) respectively. It is found that the presence of rotational speed enhances the stability of FGM plate. The centrifugal force is increases due to increasing in rotational speed. As a results the effective stiffness increase and hence the dynamic stability of FGM plate is enhanced.

Fig. 11(b) Effect of rotating speed parameter (λ = 0, 0.5, 1) on second mode instability regions of rotating FGM plate.

CONCLUSIONS

Natural frequency and dynamic stability analysis of rotating cantilever FGM plate is carried out using finite element approach. The material constituents of FGM are very along the thickness direction of the plate using power law. The governing equation of motion obtained from the Hamilton's principle and it is solved by finite element method. Stable and instable regions are obtained using Bolton theory. The effect of property distribution, thickness ratio, radius of hub and rotation on natural frequency and parametric instability is studied. The fundamental natural frequency parameter of rotating plate is decreased

by rise of power law index value. Rise of rotational speed rise the frequency parameter of FGM plate.

The increasing power law index of FGM plate is found to reduce the stability, also found that the instability occurs at lower excitation frequency ratio. The increase in hub radius and rotational speed of cantilever FGM plate rise their frequencies and dynamic stability also enhanced.

REFERENCES:

1. Amit Karmakar, and Sinha, P. K., (1997), Finite Element Free Vibration Analysis of Rotating Laminated Composite pretwisted Cantilever Plates, Journal of Reinforced Plastics and Composites. 16, 1461 -1491.
2. Bolotin, V.V., (1962), The dynamic stability of elastic systems volume I, Report, Aerospace Corporation, EI Segundo, California.
3. Chih-Ping, W. and Hao-Yuan, L., (2014), Three-dimensional free vibration analysis of functionally graded carbon nanotube-reinforced composite plates with various boundary conditions, Journal of Vibration and Control. 20, 1-19.
4. Efraim, E. and Eisenberger, M., (2007), Exact vibration analysis of variable thickness thick annular isotropic and FGM plates, Journal of Sound and Vibration. 299, 720-738.
5. Hashemi, S.H., Farhadi, S., Carra, S., (2009), Free vibration analysis of rotating thick plates, Journal of Sound and Vibration. 323, 366–384.
6. Hesham Hamed, I. and Mohammad, T., (2010), Limit-cycle Oscillations of Functionally Graded Material Plates Subject to Aerodynamic and Thermal Loads, Journal of Vibration and Control. 16, 2147-2166.
7. Hosseini-Hashemi, Sh., Fadaee, M., Atashipour, S.R., (2011), A new exact analytical approach for free vibration of Reissner–Mindlin functionally graded rectangular plates, International Journal of Mechanical Sciences. 53, 11–22.
8. Hosseini-Hashemi, Sh., Fadaee, M., Atashipour, S.R., (2011), Study on the free vibration of thick functionally graded rectangular plates according to a new exact closed-form procedure, Composite Structures. 93, 722–735.
9. Jayaram, M., Shishir, K. S. and Pravat, K. P., (2015), Parametric instability of delaminated composite plates subjected to periodic in-plane loading, Journal of Vibration and Control. 21(3), 419-434.
10. Mohammad, T. and Singh, B.N, (2010), Static response and free vibration analysis of FGM plates using higher order shear deformation theory, Applied mathematical modelling. 34, 3991-4011.
11. Ramamurti, V. and Kielb, R., (1984), Natural Frequencies of Twisted Rotating Plates, Journal of Sound and Vibration. 97 (3), 429-449.
12. Ramu I, (2015), On the dynamic stability of functionally graded material plate under parametric excitation, National Institute of Technology-Rourkela, India.
13. Ramu, I. and Mohanty, S.C., (2017), Free vibration analysis of rotating FGM plates in high thermal environment using the finite element method, International Journal of Acoustics and Vibration. 22 (1),58-67.
14. Saeidifar, M. and Ohadi, A.R., (2011), Bending vibration and buckling of non-uniform plate with time-dependent boundary conditions, Journal of Vibration and Control. 17, 1371-1393.
15. Saha, K. N., Misra, D., Pohit, G., Ghosal, S., (2004), Large Amplitude Free Vibration Study of Square Plates under Different Boundary Conditions through a Static Analysis, Journal of Vibration and Control. 10, 1009-1028.
16. Samsam Shariat, B.A., Javaheri, R., Eslami, M. R., (2005), Buckling of imperfect functionally graded plates under in-plane compressive loading, Thin-Walled Structures. 43, 1020–1036.
17. Sreenivasa murthy, S. and Ramamurti, V., (1981), Coriolies effect on the vibration of flat rotating low aspect ratio cantilever plates, The Journal of Strain Analysis for Engineering Design. 16, 97-106.
18. Talha, M. and Singh, B. N., (2011), Thermo-mechanical induced vibration characteristics of shear deformable functionally graded ceramic- metal plates using finite element method, Proceedings of the Institution of Mechanical Engineers, Part C: Journal of Mechanical Engineering Science. 225, 50-65.
19. Wang, J.T.S., Shaw, D. and Mahrenholtz, O., (1987), Vibration of rotating rectangular plates, Journal of Sound and Vibration. 112(3), 455-468.
20. Yoo, H. H. and Kim, S. K., (2002), Flapwise bending vibration of rotating plates, International Journal for Numerical Methods in Engineering. 55, 785–802.
21. Yoo, H. H. and Pierre, C., (2003), Modal characteristic of a rotating rectangular cantilever plate, Journal of Sound and Vibration. 259(1), 81–96.
22. Yoo, H. H., Park, J. H. and Park, J., (2001), Vibration analysis of rotating pre-twisted blades, Computers and structures. 79, 1811-1819.
23. Zhang, D. and Zhou, Y., (2008), A theoretical analysis of FGM thin plates based on physical neutral surface, Computational Materials Science. 44, 716–720.
24. Zhao, X., Lee, Y.Y., Liew, K.M., (2009), Free vibration analysis of functionally graded plates using the element-free kp-Ritz method, Journal of Sound and Vibration. 319, 918–939.
25. Zhao, X., Lee, Y.Y., Liew, K.M., (2009), Mechanical and thermal buckling analysis of functionally graded plates, Composite Structures. 90, 161–171.